

## Strength reduction produced by shallow notches: an asymptotic matching approach

Pietro Cornetti<sup>1,a</sup>, David Taylor<sup>2,b</sup> and Alberto Carpinteri<sup>1,c</sup>

<sup>1</sup>Department of Structural Engineering and Geotechnics, Politecnico di Torino, Turin, Italy

<sup>2</sup>Department of Mechanical and Manufacturing Engineering, Trinity College, Dublin, Ireland

<sup>a</sup>pietro.cornetti@polito.it, <sup>b</sup>dtaylor@tcd.ie, <sup>c</sup>alberto.carpinteri@polito.it

**Keywords:** Multiscale analysis, asymptotic matching, V-notches, finite fracture mechanics.

**Abstract.** Fracture in quasi-brittle material specimens with V-notches is satisfactorily described assuming as governing parameter the generalized (or notch) stress intensity factor, whose anomalous physical dimensions depend on the notch opening angle. Its critical value, i.e. the generalized toughness, can then be linked to the material strength and toughness according to a number of fracture criteria available in the literature. However, all these criteria provide an infinite failure load as the notch depth tends to zero, this undesirable property being shared with LEFM. Aim of the present paper is to overcome this shortcoming. The analysis of the notched specimens is carried out by means of a multiscale approach according to which the problem is solved separately in the region far away from the notch (the outer field) and in the region close to the notch (the inner field). Hence the asymptotic matching technique can be exploited to achieve the overall solution. The results are finally compared with experiments performed on polystyrene specimens.

### Introduction

When dealing with brittle or quasi-brittle materials, two main failure criteria are generally taken into account. The former is a stress criterion: i.e. failure takes place if, at least in one point, the maximum principal stress reaches the tensile strength  $\sigma_u$ . The latter is an energetic criterion: it states that failure happens if the crack driving force  $\mathcal{G}$  equals the crack resistance  $\mathcal{G}_F$ .  $\mathcal{G}_F$  is the so-called fracture energy, i.e. the energy necessary to create the unit fracture surface. According to Irwin's relationship and dealing, for the sake of simplicity, only with mode I crack propagation, the energetic criterion can be expressed equivalently in terms of stress intensity factor (SIF)  $K_I$  and fracture toughness  $K_{Ic}$ : failure is achieved whenever  $K_I = K_{Ic}$ . This is the failure criterion provided by linear elastic fracture mechanics (LEFM).

The stress criterion provides good results only for crack-free bodies, whereas the energetic criterion works only for bodies containing a sufficiently large crack. Otherwise both the criteria fail. Consider, on the other hand, specimens with re-entrant corners (i.e. V-notched specimens, with notch opening angle  $\omega$ ). Since the stress field is singular at notch tip, the stress criterion provides always a vanishing failure load. On the other hand, LEFM gives an infinite failure load since the order of the singularity is lower than 1/2 (which implies a null SIF). It is therefore argued that the stress and the energy aspects have to be contemporaneously considered to have a general failure criterion [1].

The goal of coupling the two approaches is usually achieved by means of the cohesive crack model [2]. It is a model widely spread in the scientific community, since it represents a very versatile tool when dealing with quasi-brittle materials. However, it requires a specific numerical algorithm to be inserted in structural design codes (see [3] for applications of the cohesive crack model to V-notches).

On the other hand, analytical or semi-analytical results may be obtained assuming that crack initiation occurs by a finite crack advancement. This kind of approach is usually named Finite Fracture Mechanics (FFM) and already applied to V-notch by Leguillon [4] and Carpinteri et al. [5].

Different versions of the FFM exist. The simplest one is achieved assuming a fixed crack advancement  $\Delta$ , i.e.  $\Delta$  is a material parameter. Fracture initiation will occur whenever the strain energy release  $\Delta\Phi$  reaches the critical value  $G_F \Delta$  [6,7]:

$$\Delta\Phi = G_F \Delta = \frac{K_{Ic}^2}{E'} \Delta \quad \text{with} \quad \Delta = \frac{2}{\pi} \frac{K_{Ic}^2}{c^2 \sigma_u^2} \quad (1)$$

where  $E'$  is the Young modulus in plane strain elastic problems. The coefficient  $c$  is equal to 1.12 for edge cracks. Application of the FFM criterion (1) to V-notched specimens results in the following failure criterion:

$$K_I^* = K_{Ic}^* \quad (2)$$

where  $K_I^*$  is the generalized SIF (sometimes referred to as notch-SIF) and  $K_{Ic}^*$  the generalized fracture toughness. The criterion (2) was already available in the literature since the pioneering work by Carpinteri [1]. According to Eq. 1, the following expression of the generalized fracture toughness is finally achieved:

$$K_{Ic}^* = \xi \frac{K_{Ic}^{2(1-\lambda)}}{\sigma_u^{1-2\lambda}} \quad (3)$$

where  $\lambda(\omega)$  is the exponent characterizing the stress field singularity according to the classical analysis due to Williams;  $\xi(\omega)$  is a parameter whose analytical expression can be found in Carpinteri et al. [5] and is based on interpolation functions from Murakami's SIF handbook. Note that  $\frac{1}{2} \leq \lambda \leq 1$  and  $\xi = 1$  for  $\omega = 0^\circ$  or  $180^\circ$ , so that Eq. 3 provides  $K_{Ic}^* = K_{Ic}$  for  $\omega = 0^\circ$  ( $\lambda = \frac{1}{2}$ ) and  $K_{Ic}^* = \sigma_u$  for  $\omega = 180^\circ$  ( $\lambda = 1$ ). Note that, in the literature, failure criteria other than Eq. 1 are available: they yield estimates of the generalized fracture toughness that differ from Eq. 3 because of different  $\xi$  values [4,5,8,9,10,11].

However, Eq. 2 presents the same drawback shown by LEFM for cracks: it provides infinite failure loads for notch depths tending to zero, since  $K_I^*$  tends to zero. Therefore the criterion (2) has to be considered valid only for large V-notches. The prediction of the failure load of specimens containing shallow V-notches is the subject of the present paper and will be obtained by means of the FFM criterion (1) together with a two-scale asymptotic analysis of the geometry involved. The asymptotic analysis will be addressed following the procedure outlined in [12], where it was exploited to analyse the blunting effect of the notch root radius in ceramic materials.

### Perturbation theory and asymptotic matching

By decomposing a tough problem into a number of relatively easy ones, perturbation theory aims to obtain approximate solutions to problems involving a small parameter  $\varepsilon$ .

Perturbations can be regular or singular. A basic feature of all regular perturbation problems is that the exact solution for small but nonzero  $\varepsilon$  smoothly approaches the solution of the unperturbed ( $\varepsilon = 0$ ) problem. Referring to differential equations, a singularly perturbed differential equation is usually related to the presence of the parameter  $\varepsilon$  in front of the highest order derivative. The solutions of such equations are characterized by the presence of a boundary layer, i.e. a narrow region where the solution changes rapidly and whose thickness approaches 0 as  $\varepsilon \rightarrow 0$ .

If an analytical solution is not achievable, an approximate solution can be obtained by dividing the interval on which the boundary-value problem is posed into two overlapping subintervals, the inner (where the boundary layer takes place) and outer domain. The solution can be computed in each interval up to some extent: missing terms are determined by imposing that a region must exist where the two solutions overlap. This technique is named asymptotic matching procedure and allows one to achieve the final (approximate) solutions [4].

In what follows, the asymptotic matching will be applied to study the effect of shallow notches. In such a case, the notch itself will be considered as a small perturbation of size  $e$  (Fig. 1). As can be easily argued, the perturbation is singular since a stress intensification/concentration is present as far as  $e \neq 0$ , whereas it suddenly disappears as the notch vanishes ( $e = 0$ ).

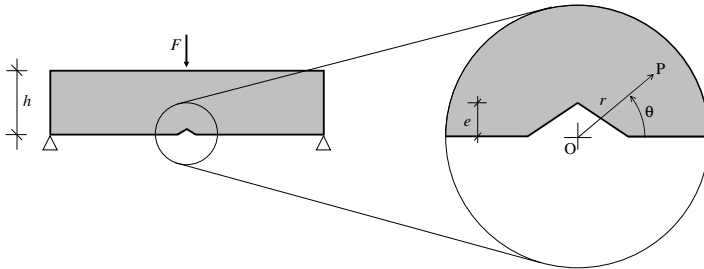


Figure 1. Three point bending test of a specimen with a shallow sharp V-notch.

### Asymptotic analysis of a notched specimen

Let us consider a specimen with a small notch loaded in mode I conditions, as is, for instance, the three point bending specimen represented in Fig. 1. We assume that the notch depth  $e$  is small with respect to the other geometrical dimensions.

What follows is based on a two-scale asymptotic analysis in plane strain linear elasticity. The actual displacement field is denoted by  $\underline{U}^e$ , where the superscript  $e$  reminds the dependence of the displacement field on the notch. Denoting by  $(r, \theta)$  the polar coordinates of a system centred at the specimen mid span intrados (see Fig. 1), the actual solution can be expressed as:

$$\underline{U}^e(r, \theta) = \underline{U}^0(r, \theta) + \text{small correction} \tag{4}$$

where  $\underline{U}^0$  is the solution of the plain, un-notched specimen (i.e. when  $e = 0$ ). As  $r$  tends to zero, it can be expanded as:

$$\underline{U}^0(r, \theta) = \underline{U}^0(r = 0) + \sigma_N r \underline{u}(\theta) + \dots \tag{5}$$

The first term at the right-hand side represents the irrelevant rigid translation;  $\sigma_N$  is the nominal stress, i.e. the maximum normal stress that would occur if the specimen were un-notched;  $\underline{u}(\theta)$  is a function of the angular coordinate  $\theta$  as well as of the material elastic parameter  $E', \nu'$  (not marked explicitly). Eq. 4 represents the outer field solution, since it is an approximation which breaks down in the neighbourhood of the notch.

To have a detailed description of the actual solution  $\underline{U}^e$  close to the notch, the domain is stretched by  $1/e$ . The new dimensionless radial coordinate is  $\rho = r/e$ . The notch size attains a unit measure and, as  $e \rightarrow 0$ , the inner domain becomes unbounded (see Fig. 2a). In the inner domain the actual solution is assumed to expand as follows:

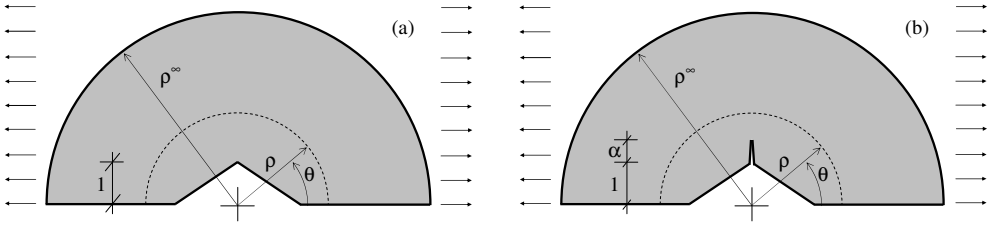


Figure 2. Inner domain and contour integral with (b) and without (a) the crack at the V-notch root.

$$\underline{U}^e(r, \theta) = \underline{U}^e(\rho, \theta) = F_0(e) \underline{V}^0(\rho, \theta) + F_1(e) \underline{V}^1(\rho, \theta) + \dots \quad (6)$$

with  $\lim_{e \rightarrow 0} F_1(e)/F_0(e) = 0$

Boundary conditions to determine the functions  $\underline{V}^i$  are needed. These conditions can be derived by the asymptotic matching, i.e. an intermediate region exists where the two expansions (the outer, Eq. 4, and the inner, Eq. 6) holds true. In other words, expression (6) for  $\rho \rightarrow \infty$  must coincide with Eq. 4 for  $r \rightarrow 0$  (i.e. with Eq. 5). This is true if:

$$F_0(e) = 1, F_1(e) = \sigma_N e, \underline{V}^0(\rho = 0) = \underline{U}^0(r = 0) \quad (7)$$

and

$$\underline{V}^1(\rho, \theta) = \rho \underline{u}(\theta) \text{ for } \rho \rightarrow \infty. \quad (8)$$

Substituting Eqs. 7,8 into Eq. 6, finally yields:

$$\underline{U}^e(r, \theta) = \underline{U}^e(\rho e, \theta) = \underline{U}^0(r = 0) + \sigma_N e \underline{V}^1(\rho, \theta) + \dots \quad (9)$$

In order to apply the finite fracture mechanics criterion of Eq. (1), we need to evaluate the displacement field when a small crack  $a$  is present at the notch root (see Fig. 2b). The ratio of the crack length to the notch depth  $e$  is denoted by  $\alpha = a/e$ . We can follow the same procedure outlined before to get the following expansion:

$$\underline{U}^e(r, \theta, a) = \underline{U}^e(\rho e, \theta, \alpha a) = \underline{U}^0(r = 0) + \sigma_N e \underline{V}^1(\rho, \theta, \alpha) + \dots \quad (10)$$

Eq. 10 generalizes Eq. 9, when  $\alpha \neq 0$ ; hence, thereafter we rewrite  $\underline{U}^e(r, \theta)$  and  $\underline{V}^1(\rho, \theta)$  as  $\underline{U}^e(r, \theta, 0)$  and  $\underline{V}^1(\rho, \theta, 0)$  respectively.

As stated in the introduction, the great advantage of this approach is that  $\underline{V}^1(\rho, \theta, \alpha)$  is independent of the applied load, geometry and notch size.  $\underline{V}^1(\rho, \theta, \alpha)$  can be computed by a finite element analysis (FEA). Since the inner domain is unbounded, we need to bound it artificially by limiting the radial coordinate at  $\rho = \rho^\infty$ ;  $\rho^\infty$  has to be large if compared with the dimensionless notch size (i.e. unity) and crack length (i.e.  $\alpha$ ). In our numerical simulation, we assumed  $\rho^\infty = 200$ . For what concerns the boundary condition (8) on the  $\rho^\infty$ -circumference, one can choose Dirichlet as well as Neumann conditions:

$$\underline{V}^1(\rho, \theta) = \rho \underline{u}(\theta) \text{ or } \underline{\sigma}[\underline{V}^1(\rho, \theta)] \underline{n} = \begin{pmatrix} \cos^2 \theta \\ -\cos \theta \sin \theta \end{pmatrix} \quad (11)$$

where  $\underline{\sigma}[\underline{V}^1]$  denotes the Cauchy stress tensor associated to the displacement field  $\underline{V}^1$  and  $\underline{n}$  the normal to the boundary. In the numerical simulations we used Neumann boundary conditions.

### The strain energy release

The strain energy release produced by a short crack  $a$  at the notch root (Fig. 2b) may be computed by a suitable application of Betti's theorem.

Let us consider a region surrounding the notch, e.g., for the sake of simplicity, bounded by a circumference of radius  $r$  (see Fig. 2, dashed line). Then, consider two configurations: the former one without the crack of length  $a$  at the notch root (denoted by "c", since the crack is closed, Fig. 2a); the latter one with the crack (denoted by "o", since the crack is open, Fig. 2b). The configuration without the crack can be seen as if the crack were open but with a stress distribution acting on the crack lips corresponding to the closed geometry. Betti's theorem states that the reciprocal works of the two systems are equal:

$$\int_0^\pi \underline{t}_o \cdot \underline{\eta}_c \, r d\theta = \int_0^\pi \underline{t}_c \cdot \underline{\eta}_o \, r d\theta + \int_0^a \underline{\sigma}_c \times (\eta_x)_o \, dy \quad (12)$$

where  $\underline{t}$  is the stress vector acting on the boundary,  $\underline{\eta}$  the displacement field and a dot ( $\cdot$ ) represents the scalar product. Since only mode I loading conditions have been considered, only the normal component  $\sigma$  of the stress and the horizontal displacement  $\eta_x$  appear in the second integral at the right-hand side ( $x, y$  being the horizontal and vertical axes, respectively). It is easily recognized that this term is twice the crack closure work, i.e. the strain energy release  $\Delta\Phi$  due the crack formation. Therefore:

$$\Delta\Phi = \frac{1}{2} \int_0^\pi (\underline{t}_o \cdot \underline{u}_c - \underline{t}_c \cdot \underline{u}_o) \, r d\theta \quad (13)$$

From Eq. 13 we see that the integral at the right-hand side does not depend on  $r$ , i.e. is a path-independent integral. According to the notation used in the previous section, Eq. 13 may be rewritten as:

$$\Delta\Phi = \frac{1}{2} \int_0^\pi \{ \underline{\sigma}[\underline{U}^e(r, \theta, a)] \underline{n} \cdot \underline{U}^e(r, \theta, 0) - \underline{\sigma}[\underline{U}^e(r, \theta, 0)] \underline{n} \cdot \underline{U}^e(r, \theta, a) \} \, r d\theta \quad (14)$$

Taking the integral in the inner domain, i.e. using the expansions (9) and (10), yields:

$$\Delta\Phi = \frac{\sigma_N^2}{2E'} e^2 \int_0^\pi \{ \underline{\sigma}[\underline{V}^1(\rho, \theta, \alpha)] \underline{n} \cdot \underline{V}^1(\rho, \theta, 0) - \underline{\sigma}[\underline{V}^1(\rho, \theta, 0)] \underline{n} \cdot \underline{V}^1(\rho, \theta, \alpha) \} \, \rho d\theta \quad (15)$$

The contour integral at the right-hand side depends only on the dimensionless parameter  $\alpha$  (and on the notch shape). In fact: (i) it does not depend on the material parameter  $E', \nu'$  (since  $\underline{V}^1 \propto 1/E'$  and

a numerical check shows that Poisson coefficient has no influence); (ii)  $\theta$  disappears by integration; (iii)  $\rho$  does not affect the integral since it is path-independent; (iv) the integral is independent of the size of the perturbation (i.e. the notch) and of the load thanks to the asymptotic matching technique used above. The information about the load, the material and the notch size are collected in the term  $(\sigma_{N,e})/2E'$  multiplying the integral in Eq. 15, which will be hereafter denoted by  $I(\alpha)$ .

$\alpha$	$I(\alpha)$	$\sigma_{N,f} / \sigma_u$ (Eq. 17)	$\sigma_{N,f} / \sigma_u$ (Eq. 19)
0	0	0	0
0.5	4.553	0.4658	0.4690
1	11.47	0.5871	0.6121
2	31.33	0.7103	0.7989
4	95.71	0.8127	1.0428
$\infty$	$\infty$	1	$\infty$

Table 1. Values of the path-independent integral and of the residual strength fraction for different values of  $\alpha$ .

### The failure criterion

Let us apply the FFM criterion of Eq. 1. By means of Eq. 15 it becomes:

$$\frac{(\sigma_{N,f} e)^2}{2E'} I(\alpha) = \frac{K_{Ic}^2}{E'} \Delta \quad (16)$$

where the subscript  $f$  has been introduced since now the nominal stress corresponds to the value at incipient failure and  $\alpha = \Delta/e$ . By some analytical manipulations, we finally get:

$$\frac{\sigma_{N,f}}{\sigma_u} = c \alpha \sqrt{\frac{\pi}{I(\alpha)}} \quad (17)$$

Once the relation between load and nominal stress is known, Eq. 17 provides also the failure load. The ratio (17) is always smaller than unity. It can be seen as the strength reduction caused by the presence of the notch, since it is the ratio between the strengths with and without the notch.

Eq. 17 is a very general result, the only limitation being that both the crack advance ( $\Delta$ ) and the notch size  $e$  have to be much smaller than the specimen size. In other words, Eq. 17 is valid for specimens containing *shallow* notches subject to *mode I* loading conditions (opening).

Once  $\underline{V}^1(\rho, \theta, \alpha)$  is obtained by a FEA, the contour integral  $I(\alpha)$  can be easily computed. In Table 1, its value as well as the value of the ratio (17) are given for different values of the geometrical-material parameter  $\alpha$  ( $0 < \alpha < \infty$ ) in the case of V-notches with opening angle  $\omega = 120^\circ$ .

Concerning the limit cases, it should be noted that, for  $\alpha \rightarrow \infty$ , i.e. for notch size tending to zero and/or relatively ductile materials, the structure becomes insensitive to the notch and the nominal stress at failure coincides with the ultimate tensile strength as anticipated in [1]. This result is valid for any notch shape.

For  $\alpha \rightarrow 0$ , i.e. for large notch size and/or very brittle materials, the result depends on the notch shape. Let us consider the case of a V-notch. If  $\alpha \rightarrow 0$ , the failure conditions are achieved when the generalized SIF reaches its critical value (Eq. 2). However, since we assumed that the notch depth is much smaller than the structural size, the generalized SIF has the following expression:

$$K_I^* = \beta \sigma_N e^{1-\lambda} \quad (18)$$

where  $\beta$  is a parameter depending on the notch opening angle: for instance,  $\beta = 1$  for  $\omega = 180^\circ$  ( $\lambda = 1$ , flat edge) and  $\beta = c\sqrt{\pi}$  for  $\omega = 0^\circ$  ( $\lambda = 1/2$ , edge crack). A numerical simulation can provide the values for intermediate cases: for instance,  $\beta = 2.13$  for  $\omega = 120^\circ$ . By means of Eqs. 2,3 and 18, we finally get the following limit value:

$$\frac{\sigma_{N,f}}{\sigma_u} = \xi \left( \frac{\pi c^2 \alpha}{2} \right)^{1-\lambda}, \quad \alpha \rightarrow 0 \tag{19}$$

Eq. 19 is tabulated in Table 1 as well. As expected, it provides a good approximation to Eq. 17 for  $\alpha \rightarrow 0$ , whereas it yields an overestimation of the structural strength as the notch becomes smaller and smaller. In the limit of a vanishing notch ( $\alpha \rightarrow \infty$ ), Eq. 19 provides an infinite failure load; as stated in the introduction, this is a shortcoming shared with LEFM, since Eq. 19 derives from Eq. 2.

The strength predictions given by Eqs. 17 and 19 are plotted in Fig. 3a vs.  $1/\alpha$ , i.e. the dimensionless notch size ( $e/\Delta$ ). Also in this plot it is evident that the LEFM-like criterion  $K_I^* = K_{Ic}^*$  may largely overestimate the failure load in the case of very small notches. In Fig. 3b the same diagram is plotted in a bi-logarithmic scale. In such a case, Eq. 19 is represented by a straight line of negative slope ( $1-\lambda$ ): the prediction of the present model departs from this straight line for large  $\alpha$  values. Finally, it is worth noting that figs.3 describe the effect of the notch size and not the size effect, since the structural size is assumed to be constant and much larger than both the notch and the crack advancement.

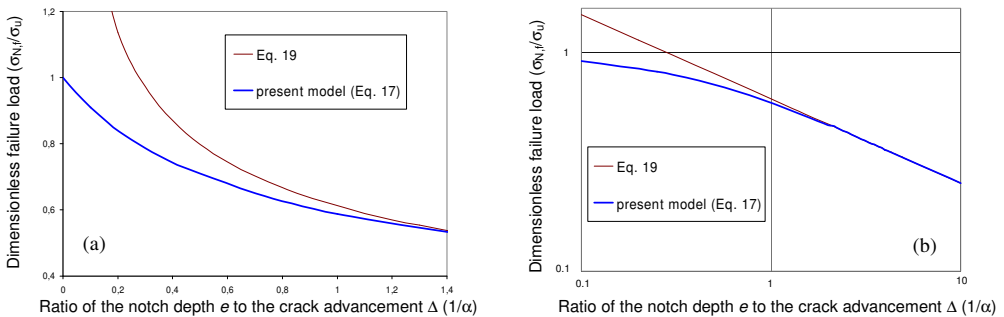


Figure 3. Dimensionless failure load vs.  $\alpha^{-1}$ (a). Bi-logarithmic plot (b).

### Comparison with experimental data

The predictions provided by the present model were compared with the data obtained by a series of three point bending tests. The specimens were made of Polystyrene and presented at the mid-span a sharp V-notch with opening angle equal to  $120^\circ$  (the notch root radius was kept smaller than  $10\mu\text{m}$ ). The relative notch depths were taken equal to: 0, 1/90, 1/30, 1/10. Each geometry was tested five times. The un-notched specimens provided an average value of the tensile strength  $\sigma_u$  equal to 70.6 MPa, whereas the fracture toughness was derived by previous tests performed on cracked specimens of the same material and stock, yielding  $K_{Ic} = 2.23 \text{ MPa}\sqrt{\text{m}}$ . Thus the crack advancement  $\Delta$  is equal to 506  $\mu\text{m}$ . For details about the geometries tested see [5].

By definition, the ratio of the recorded failure loads to the average failure load of the un-notched specimens is also equal to the ratio of the nominal stress at failure to the tensile strength. Hence the results are drawn in Fig. 4, where experimental data and theoretical predictions have been plotted vs. the relative notch depth. It is evident the excellent agreement for small notches, where the LEFM-like criterion breaks down [1]. On the other hand, the asymptotic approach underestimates

the strength for relatively large notch depths (i.e. 1/10), but this feature had to be expected since the perturbation theory breaks down when the smallness assumption fails. However, for large notches, Eq. 3 provides excellent results if the generalized SIF is properly computed (see [5]). In other words, Eq. 19 never gives satisfactory results, either because it does not consider correctly the effect of shallow notches either because the asymptotic value of the generalized SIF (18) does not hold true for notches whose size is comparable with the specimen height.

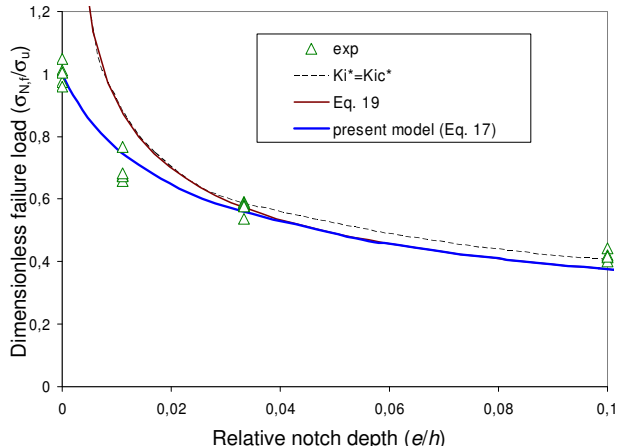


Figure 4. Dimensionless failure load vs. relative notch depth: comparison with experimental data.

## Conclusions

In the present paper a multiscale analysis was developed to estimate the strength decrement due to the presence of a shallow notch. The analysis is applicable to any notch shape and geometry, provided that the notch is subject to mode I loading conditions. Numerical results were explicitly given for specimens with a re-entrant corner of 120°. A fairly good agreement with experimental data seems to prove the soundness of the present approach.

## References

- [1] A. Carpinteri: Engng Fract Mech. Vol 26 (1987), p. 143–155.
- [2] A. Carpinteri: J Mech Phys Solids. Vol 37 (1989), p. 567–582.
- [3] F. Gómez and M. Elices: Engng Fract Mech. Vol 70 (2003), p. 1913–1927.
- [4] D. Leguillon: Eur J Mech A/Solids. Vol 21 (2002), p. 61–72.
- [5] A. Carpinteri, P. Cornetti, N. Pugno, A. Sapora and D. Taylor: Engng Fract Mech. Vol 75 (2008), p. 1736–1752.
- [6] N. Pugno and N. Ruoff: Philos Mag A. Vol 84 (2004), p. 2829–2845.
- [7] D. Taylor, P. Cornetti and N. Pugno: Engng Fract Mech. Vol 72 (2005), p. 1021–1038.
- [8] P. Lazzarin and R. Zambardi: Int J Fracture. Vol 112 (2001), p. 275–298.
- [9] A. Seweryn: Engng Fract Mech. Vol 47 (1994), p.673–681.
- [10] G. C. Sih and J.W. Ho: Theor Appl Fract Mec. Vol 16 (1991), p. 179-214.
- [11] A. Carpinteri, N. Pugno: Engng Fract Mech. Vol 72 (2005), p. 1254–1267.
- [12] D. Picard, D. Leguillon and C. Putot: J Eur Ceram Soc. Vol 26 (2006), p. 1421–1427.